

Searching for gap zeros in Sr_2RuO_4 via field-angle-dependent specific-heat measurement

Shunichiro KITAKA^{1*}, Shota NAKAMURA^{1†}, Toshiro SAKAKIBARA¹, Naoki KIKUGAWA², Taichi TERASHIMA²,
Shinya UJI^{2,3}, Dmitry A. SOKOLOV⁴, Andrew P. MACKENZIE⁴, Koki IRIE⁵, Yasumasa TSUTSUMI^{6,7},
Katsuhiko SUZUKI⁸, and Kazushige MACHIDA⁵

¹*Institute for Solid State Physics, University of Tokyo, Kashiwa, Chiba 277-8581, Japan*

²*National Institute for Materials Science, 3-13 Sakura, Tsukuba, Ibaraki 305-0003, Japan*

³*Graduate School of Pure and Applied Sciences, University of Tsukuba, Tsukuba, Ibaraki 305-8577, Japan*

⁴*Max Planck Institute for Chemical Physics of Solids, Nothnitzer Str. 40, 01187 Dresden, Germany*

⁵*Department of Physics, Ritsumeikan University, Kusatsu, Shiga 525-8577, Japan*

⁶*Department of Basic Science, The University of Tokyo, Meguro, Tokyo 153-8902, Japan*

⁷*Condensed Matter Theory Laboratory, RIKEN, Wako, Saitama 351-0198, Japan*

⁸*Research Organization of Science and Technology, Ritsumeikan University, Kusatsu, Shiga 525-8577, Japan*

The gap structure of Sr_2RuO_4 , which is a longstanding candidate for a chiral p -wave superconductor, has been investigated from the perspective of the dependence of its specific heat on magnetic field angles at temperatures as low as 0.06 K ($\sim 0.04T_c$). Except near H_{c2} , its fourfold specific-heat oscillation under an in-plane rotating magnetic field is unlikely to change its sign down to the lowest temperature of 0.06 K. This feature is qualitatively different from nodal quasiparticle excitations of a quasi-two-dimensional superconductor possessing vertical lines of gap minima. The overall specific-heat behavior of Sr_2RuO_4 can be explained by Doppler-shifted quasiparticles around horizontal line nodes on the Fermi surface, whose in-plane Fermi velocity is highly anisotropic, along with the occurrence of the Pauli-paramagnetic effect. These findings, in particular, the presence of horizontal line nodes in the gap, call for a reconsideration of the order parameter of Sr_2RuO_4 .

Sr_2RuO_4 , a layered-perovskite superconductor with $T_c=1.5$ K,¹⁾ has attracted enormous attention ever since Knight-shift experiments provided favorable evidence that it exhibits spin-triplet pairing.²⁻⁵⁾ Numerous experiments have demonstrated that Sr_2RuO_4 has non s -wave properties,^{6,7)} and some of the experimental reports indicate a degenerate order parameter.^{8,9)} The simple Fermi-surface topology of Sr_2RuO_4 comprising of three cylindrical sheets (α , β , and γ)^{10,11)} together with its well-characterized Fermi-liquid behavior has led to the construction of several theoretical models to describe superconductivity.⁶⁾ Among these models, a spin-triplet chiral p -wave pairing characterized by $\mathbf{d} = \Delta_0 \hat{\mathbf{z}}(k_x \pm ik_y)$ has been considered to be a promising candidate.

However, several experimental facts exist that cannot be explained in the framework of this spin-triplet scenario.¹²⁾ A serious controversy is the mechanism of the first-order superconducting transition along with the H_{c2} limit induced by the in-plane magnetic field.¹³⁻¹⁶⁾ It is reminiscent of the Pauli-paramagnetic effect that is not allowed in the spin-triplet scenario. The superconducting gap structure of Sr_2RuO_4 is also a contentious issue. In general, a chiral p -wave gap opening on the cylindrical Fermi-surface sheets has no symmetry-protected node. Nevertheless, the gap amplitude of Sr_2RuO_4 has been widely accepted to be modulated, and lines of deep minima (or nodes) are suggested to be present somewhere in the gap because of the power-law temperature dependence of various physical quantities.¹⁷⁻²⁰⁾ Furthermore, universal heat

transport has raised the possibility of a nodal gap.¹⁸⁾ Various gap structures including vertical and horizontal line node gaps have been proposed so far;²¹⁻²⁵⁾ however, the location of gap minima has not yet been established.

During this decade, field-angle-dependent measurements that probe quasiparticle density of states, $N(E)$, have been developed as powerful tools for determining the position of gap zeros.²⁶⁻²⁹⁾ This technique takes advantage of the Doppler energy shift, $\delta E = m_e v_F \cdot v_s$, of $N(E)$ in the mixed state. Here, m_e is the effective mass, v_F is the Fermi velocity, and v_s ($\perp \mathbf{H}$) is the velocity of the supercurrent circulating around vortices. If the gap has zeros somewhere on the Fermi surface, $N(E=0)$ becomes finite in those areas because of the Doppler shift and varies with the angle between the field ($\perp v_s$) and the nodal (v_F) directions. Therefore, the field-angle dependence of $N(E=0)$ provides key information about the gap structure.

In 2004, Deguchi *et al.* reported the in-plane field-angle ϕ dependence of the specific heat, $C(\phi)$, of Sr_2RuO_4 in the temperature range $0.12 \leq T \leq 0.51$ K.^{23,24)} They proposed that the gap has fourfold anisotropy within the ab plane, *i.e.*, four vertical lines of gap minima, based on the assumption that $C(\phi) \propto N(\phi, E=0)$. However, recent theoretical studies^{28,29)} have suggested that the Doppler-predominant condition [$C \propto N(E=0)$] is restricted in the low-temperature region because $C(T)$ at a finite temperature mainly reflects $N(E)$ at $E \sim 2.4k_B T$. In other words, the reversed ϕ dependence of $N(E \neq 0)$ changes the sign of the $C(\phi)$ oscillation, *e.g.*, approximately at $0.1T_c$ in the case of quasi-two-dimensional $d_{x^2-y^2}$ -wave superconductors.^{28,29)} Such a sign change was indeed observed in nodal superconductors CeCoIn_5 ³⁰⁾ and KFe_2As_2 ,³¹⁾ though it has not yet been detected in Sr_2RuO_4 ,

*kittaka@issp.u-tokyo.ac.jp

†Present address: Department of Engineering Physics, Electronics and Mechanics, Graduate School of Engineering, Nagoya Institute of Technology, Nagoya 466-8555, Japan

at least above 0.12 K ($\sim 0.08T_c$).^{23,24)}

Here, we report the results of high-precision $C(\phi)$ measurements at temperatures as low as 0.06 K ($\sim 0.04T_c$). We reveal that, well below H_{c2} , the normalized amplitude of the $C(\phi)$ oscillation, $A_4(T, H)$, monotonically varies with T and H without a sign change. By comparing our results with microscopic calculations, we find that the observed features in $C(T, H, \phi)$ can be qualitatively reproduced by a horizontal line node gap on a Fermi-surface sheet, which exhibits a strong in-plane anisotropy in the Fermi velocity, along with the Pauli-paramagnetic effect.

High-quality single crystals of Sr_2RuO_4 were grown by a floating-zone method,³²⁾ and a single 11.2-mg piece was used. The crystal was oriented using the backscattering X-ray Laue method. The angle-resolved specific heat $C(T, H, \phi, \theta)$ was measured by the quasi-adiabatic heat-pulse method using a dilution refrigerator. Here, ϕ (θ) denotes an azimuthal (polar) field angle relative to the [100] ([001]) axis, as represented in Fig. 1(b). The addenda of our calorimeter mainly consisted of a stage (silver foil), thermometer, and heater. A ruthenium-oxide chip resistor (Panasonic, ERJ-XGNJ, 8.2 k Ω) was used as a thermometer; it was cut into thirds (resulting in reducing the resistance to 3.3 k Ω) and whose substrate was polished to reduce its heat capacity. A ruthenium-oxide chip resistor (ROHM, MCR004, 240 Ω) was used as a heater, whose substrate was also polished. In this study, we have measured the addenda heat capacity carefully and subtracted its contribution, as depicted in the lower inset of Fig. 1(b). The magnetic field was generated using a vector magnet; the field was up to 3 T along the z -axis and 5 T along the x -axis. By using a stepper motor mounting on top of the Dewar, the refrigerator could be rotated around the z -axis. Thus, the orientation of the magnetic field was controlled three-dimensionally with high accuracy (better than 0.05°).

Figure 1(a) shows the temperature dependence of C/T at 0 and 2 T in $H \parallel [100]$. In zero field, a clear specific-heat jump is observed at T_c of 1.505 K (midpoint), which is as high as the highest T_c of Sr_2RuO_4 .³³⁾ At 2 T ($H > H_{c2}$) and at low temperatures, C/T shows a gradual increase with decreasing temperature. This can be attributed to the nuclear specific heat. To explore the electronic contribution C_e , the phonon and nuclear contributions, C_{ph} and C_N , respectively, are subtracted from the data shown below. Here, the Debye temperature is 410 K, and C_N is $(0.08 + 0.14H^2)/T^2$ $\mu\text{J}/(\text{mol K})$. The latter is calculated using a nuclear spin Hamiltonian with the nuclear quadrupole resonance parameters of ^{99}Ru , ^{101}Ru , and ^{87}Sr nuclei.^{34,35)} The resulting $C_e/T = (C - C_{\text{ph}} - C_N)/T$ at 2 T still shows a slight upturn at low temperatures (not shown), implying insufficient subtraction of the non-electronic contributions. Nevertheless, we adopt this definition to avoid uncertainty.

In Fig. 1(b), C_e/T at 0.06 K is plotted as a function of H applied parallel to the [100] and [110] axes. The increase in $C_e(H)/T$ from 0 T to H_{c2} is 33 mJ/(mol K²), which is comparable to results of a previous study,²³⁾ although the absolute value is enhanced due to the difference in the definition of C_e .³⁶⁾ This fact indicates that the superconducting volume fraction of the present sample is above 90%, and that an offset of ~ 6 mJ/(mol K²) is given to C_e/T in Fig. 1(b) by the remaining non-electronic contributions. In the high-field region, $C_e(H)$ shows a single, sharp jump at $\mu_0 H_{c2}$ of 1.52 (1.56) T in

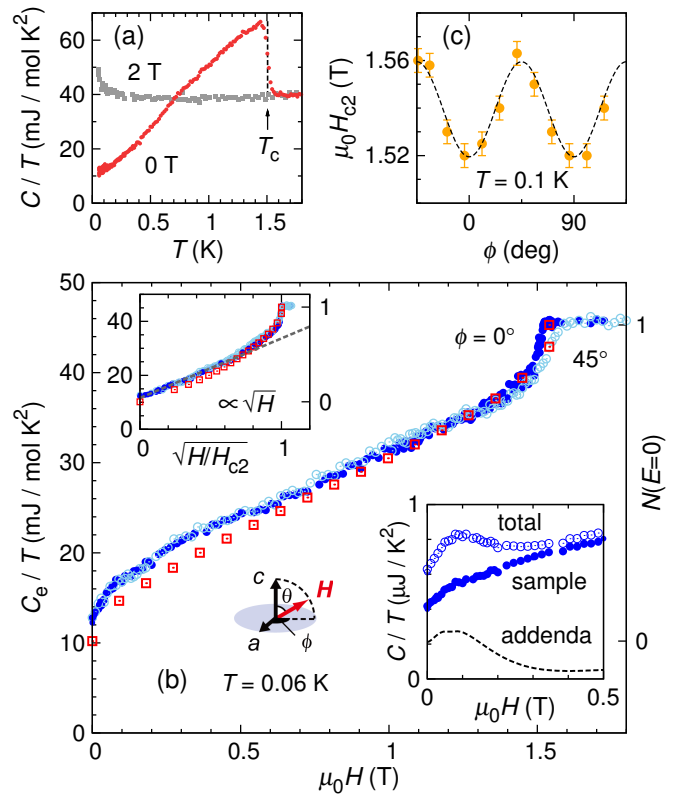


Fig. 1. (a) Temperature dependence of the specific heat divided by temperature C/T at 0 and 2 T in $H \parallel [100]$. (b) $C_e/T = (C - C_{\text{ph}} - C_N)/T$ at 0.06 K as a function of the magnetic field in $H \parallel [100]$ ($\phi = 0^\circ$; closed circles) and $H \parallel [110]$ ($\phi = 45^\circ$; open circles). Squares represent $N(E = 0)$ at $\phi = 45^\circ$ obtained by microscopic calculation assuming $\Delta(\mathbf{k}) = \Delta_0 \cos ck_z$ with $b = 0.5$ and $\mu = 0.04$ (refer to the text). The upper inset shows the same data as a function of \sqrt{H}/H_{c2} along with a linear function in \sqrt{H} (dashed line). The lower inset shows the field dependence of the addenda heat capacity (dashed line) together with total (open circles) and sample (closed circles) heat capacities (Sr_2RuO_4 ; at 0.06 K in $H \parallel [100]$). (c) In-plane upper critical field H_{c2} as a function of the azimuthal field angle ϕ at 0.1 K.

$H \parallel [100]$ ([110]). In Fig. 1(c), the in-plane H_{c2} shows four-fold anisotropy, which is consistent with the results of previous reports.^{14,37,38)} At low fields, $C_e(H)$ is nearly proportional to \sqrt{H} , as indicated with a dashed line in the upper inset of Fig. 1(b). This fine \sqrt{H} behavior supports the occurrence of low-energy quasiparticle excitations around lines of deep gap minima or nodes.³⁹⁾

In previous reports,^{17,23)} a shoulder anomaly was detected in the low-temperature $C_e(H)$ around $\mu_0 H \sim 0.15$ T, which was attributed to the abrupt suppression of minor gaps in a weakly-coupled multiband superconductor. This is similar to the cases of MgB_2 ⁴⁰⁾ and KFe_2As_2 .^{31,41)} However, no such anomaly is observed in our data after precise subtraction of the addenda contribution. It is noted that the total heat capacity shows a shoulder anomaly which can be attributed to the addenda contribution [the lower inset of Fig. 1(b)]. The lack of the multigap feature indicates relatively strong coupling between the three gaps on the α , β , and γ bands; all three gaps survive up to relatively high fields.

To examine the in-plane gap anisotropy, $C_e(\phi)$ was measured in several magnetic fields ($0.07 \leq \mu_0 H \leq 1.45$ T) that were rotated within the ab plane. The results of $C_e(\phi)/T$ at 0.06, 0.1, and 0.2 K are shown in Fig. 2(a). In the wide field range, $C_e(\phi)$ shows a clear fourfold oscillation that fits the

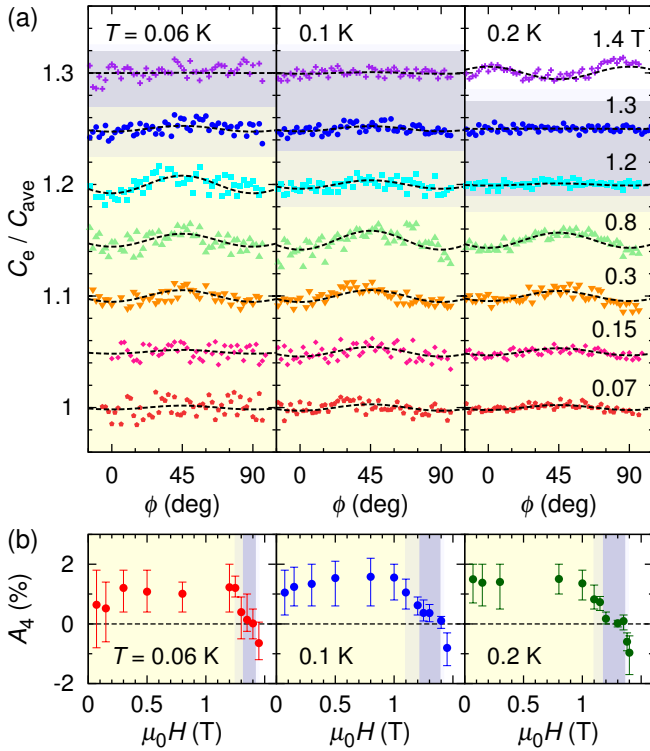


Fig. 2. Field-angle ϕ dependence of C_e/C_{ave} at 0.06, 0.1, and 0.2 K measured in a rotating magnetic field within the ab plane. Here, $C_{ave} = C_0 + C_H$ and the data are vertically shifted by 0.05 for clarity. Dashed lines are fits to the data based on the function $C = C_0 + C_H(1 - A_4 \cos 4\phi)$. Here, C_0 and C_H are zero-field and field-dependent components of C_e . (b) $A_4(H)$ obtained from the fits.

function $C_e(\phi) = C_0 + C_H(1 - A_4 \cos 4\phi)$ [dashed lines in Fig. 2(a)].⁴²⁾ Here, C_0 is the zero-field value of C_e , C_H is the field-dependent part of C_e , and A_4 is the amplitude of the fourfold oscillation normalized by C_H . In Fig. 2(b), $A_4(H)$ obtained from the fit in the entire range is plotted at each temperature along with somewhat overestimated error bars; the error bars represent minimum and maximum values of $A_4(H)$ obtained from the partial fit in the range $\phi_0 - 30^\circ \leq \phi \leq \phi_0 + 30^\circ$, where the central angle ϕ_0 is changed from 30° to 60° approximately. In the present temperature range, $A_4(H)$ stays roughly 1% below 1 T (yellow shaded area). Importantly, a sign change of A_4 is unlikely to occur at low fields; *e.g.*, A_4 including the error bars is always positive for $0.06 \text{ K} \leq T \leq 0.2 \text{ K}$ at a low field of 0.3 T. With increasing field, $A_4(H)$ suddenly decreases and becomes nearly zero around 1.3 T (blue shaded area). In high fields close to H_{c2} , the sign of $A_4(H)$ is reversed due to the anisotropy of $H_{c2}(\phi)$.

In order to explore the out-of-plane gap anisotropy, we investigated the polar-angle θ dependence of the specific heat at 0.06 K under a rotating field within the (010) plane ($\phi = 0^\circ$). As demonstrated in Supplemental Material⁴³⁾ (I), however, little information on the out-of-plane gap anisotropy can be extracted from $C_e(\theta)$ ⁴⁴⁾ because $C_e(\theta, H)$ is dominated by $H_{\parallel c}$ because of the large anisotropy ratio of the coherence length ($\xi_a/\xi_c \sim 60$).¹⁵⁾ This fact, however, suggests that the previously reported steep suppression of $A_4(\theta)$ under a conically-rotating field²⁴⁾ is not due to the compensation of antiphase gap anisotropies between active and passive bands but due to this scaling by $H_{\parallel c}$.

Let us discuss the origin of the $C_e(\phi)$ oscillation in

Sr_2RuO_4 . By combining the present $A_4(H)$ data at 0.06, 0.1, and 0.2 K with $A_4 = 0$ at 0.51 K below 0.9 T ,²³⁾ a contour plot of $A_4(T, H)$ is depicted in Fig. 3(a). Clearly, this map is very different from $A_4(T, H)$ calculated for d_{xy} - and $d_{x^2-y^2}$ -wave gaps on a rippled cylindrical Fermi surface [Fig. 3(b)].²⁹⁾ In particular, Fig. 3(b) shows a sign change of A_4 at $T \sim 0.12T_c$ in low fields below $\sim 0.3H_{c2}$. On theoretical grounds, the sign-changing line in Fig. 3(b) moves by warping the cylindrical Fermi-surface shape;⁴⁵⁾ the line is shifted toward a lower (higher) field and a lower (higher) temperature if vertical line nodes are present on large (small) curvature parts of the warped Fermi surface.⁴⁶⁾ For Sr_2RuO_4 , the quasi-two-dimensional γ band is nearly cylindrical, which yields the sign-changing line around approximately $0.1T_c$. By contrast, quasi-one-dimensional α and β bands have flat and high-curvature parts in the $\langle 100 \rangle$ and $\langle 110 \rangle$ direction, respectively. If the d_{xy} -type vertical lines of deep gap minima exist on the α and/or β bands and dominantly contribute to the $C_e(\phi)$ oscillation, the observed $A_4(T, H)$ map might be reproduced to some extent. However, this is not guaranteed because fine-tuning of multiband parameters is essential.

An alternative, more promising scenario is to assume a horizontal line node gap. According to the recent band-structure calculation,⁴⁷⁾ the in-plane v_F -anisotropy ratio, $v_{F\parallel[110]}/v_{F\parallel[100]}$, is estimated to be roughly 4 (0.8⁴⁸⁾) for the γ band (α and β bands). If the in-plane anisotropy of the Fermi velocity, $v_F(\phi_k)$, is sufficiently large, a prominent $C_e(\phi)$ oscillation is expected because of an anisotropic Doppler shift $|\delta E(\phi_k)| \propto v_F(\phi_k) |\sin(\phi - \phi_k)|$ at ϕ_k around the horizontal line nodes.⁴⁹⁾ To examine this possibility, microscopic calculations were performed by assuming a horizontal line node gap $\Delta(\mathbf{k}) = \Delta_0 \cos ck_z$ and $v_F(\phi_k) = v_{F0}(b)(1 - b \cos 4\phi_k)$ ⁴⁶⁾ on the rippled cylindrical Fermi surface; this method was similar to that used in previous reports.^{29,50,51)} Here, we use the anisotropic parameter $b = 0.5$ (for the γ band) and the Maki parameter $\mu = 0.04$; the latter is adopted to reproduce the H_{c2} limit.

The calculated result of $N(E = 0, H)$ in $H \parallel [110]$ is shown in Fig. 1(b) with squares that match $C_e(H)$ sufficiently owing to the nodal gap with the finite Maki parameter.^{52,53)} Slight mismatch at low fields can be attributed to thermal excitations of quasiparticles in C_e/T at 0.06 K which are absent in $N(E = 0)$; note that the origin of $N(E = 0)$ is vertically shifted so that in zero field $N(E = 0)$ corresponds to C_e/T at 0 K estimated by the extrapolation of the $C_e(T)$ data to 0 K. In Fig. 3(c), the calculated $A_4(H)$ (squares)^{46,54)} is compared with the experimental result at 0.1 K (circles). The absence of a sign change in $A_4(H)$ at low fields and its steep decrease in high fields are captured by this model. The latter is caused by the Pauli-paramagnetic effect; without this, $A_4(H)$ starts to decrease at a relatively low field ($\sim H_{c2}/3$) [refer to Supplemental Material⁴³⁾ (II)] and the low-temperature $C_e(H)$ behavior as well as the H_{c2} limitation cannot be reproduced. A slight mismatch above $\sim 1.2 \text{ T}$ might suggest the occurrence of an extra phase that is not considered in the present calculation. A possible one is the Fulde-Ferrell-Larkin-Ovchinnikov phase.⁵⁵⁾ This phase might be the origin of the strange $A_4(H) \sim 0$ region around 1.3 T and in-plane H_{c2} anisotropy ($H_{\parallel[100]} < H_{\parallel[110]}$) developing below 0.8 K (above 1.2 T),^{37,56)} which is inverted to the anisotropy expected from $v_F(\phi_k)$ of the γ band. Figure 3(d) shows a contour map of the

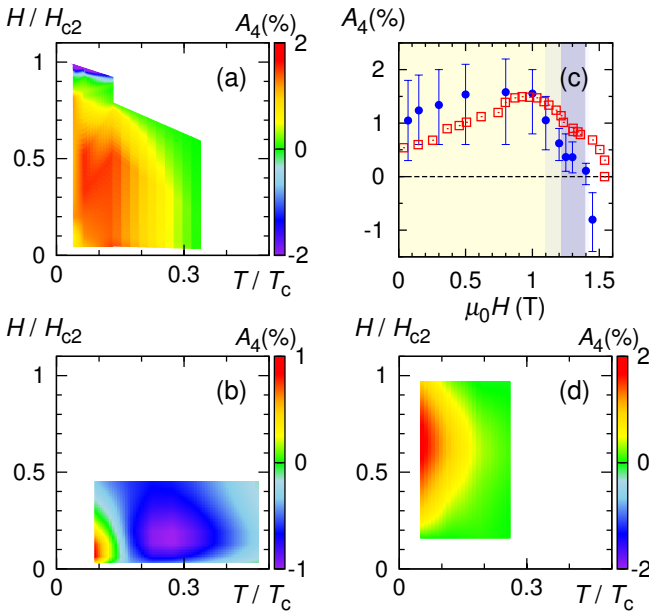


Fig. 3. (a) Contour plot of $A_4(T, H)$ made by using the present ($T/T_c \leq 0.13$) and previous ($T/T_c = 0.34, H/H_{c2} \leq 0.6$)²³ experimental data. (b) $A_4(T, H)$ calculated for a d_{xy} -wave gap with $b = 0$ and $\mu = 0.29$. $A_4(T, H)$ for a $d_{x^2-y^2}$ -wave gap is obtained by reversing the sign in (b). (c) $A_4(H)$ (squares) and (d) $A_4(T, H)$ map obtained from microscopic calculations assuming $\Delta(\mathbf{k}) = \Delta_0 \cos ck_z$ with $b = 0.5$ and $\mu = 0.04$ ^{46,54} (see text). Circles in (c) are the experimental data at 0.1 K.

calculated $A_4(T, H)$. This also reproduces no sign change and peak structure of $A_4(T, H)$ in Fig. 3(a). Thus, a horizontal line node gap can explain various features of $C_c(T, H, \phi)$ by taking into account the in-plane v_F anisotropy of the γ band⁵⁷ and the Pauli-paramagnetic effect.

The horizontal line node gap is, however, incompatible with the p - and f -wave scenarios suggested in the previous reports.^{23,25} In addition, the absence of multigap feature in $C_c(H)$, together with the good match between the experimental $C_c(H)$ and the calculated $N(E = 0)$ assuming a nodal gap on a single band, supports the presence of nodes in all three gaps, rather than only in passive bands.⁵⁸ In the tetragonal D_{4h} symmetry, several gap symmetries possessing horizontal line nodes exist, *e.g.*, $(5k_z^2 - 1)(k_x \pm ik_y)$ [E_u], $k_z(k_x \pm ik_y)$ [E_g], k_z [A_u], and $\cos(k_z c)$ [A_{1g}] in weak spin-orbit coupling (the orbital part only). The former two are broken time-reversal symmetries that are consistent with the results of μ SR and Kerr-rotation experiments.^{8,9} Non-zero residual thermal conductivity along the c axis²⁵ might support the E_u or A_{1g} symmetry, for which horizontal line nodes are located at off-centered positions. To test these gap symmetries, a spin resonance experiment using inelastic neutron scattering at $\mathbf{Q} = (1/3, 1/3, q_z)$ might be useful, *e.g.*, at $q_z = 0.15, 0.25$ and 0.35 . Notably, the absence of spin resonance at $\mathbf{Q} = (1/3, 1/3, 0)$ ⁵⁹ is also incompatible with the vertical-line-node scenario.

In summary, we have investigated the gap anisotropy of Sr_2RuO_4 from field-angle-dependent specific-heat measurements. In $H \parallel ab$, the low-field specific heat increases in proportion to \sqrt{H} with no multigap structure at 0.06 K. This suggests that multiple gaps on the α , β , and γ bands equivalently survive and possess lines of deep minima in some directions. We have revealed that the fourfold oscillation in the low-field $C_c(\phi)$ does not change its sign even at 0.06 K. In addition, an abrupt change in the normalized oscillation amplitude $A_4(H)$ is observed around $\mu_0 H \sim 1.2$ T. These features can be understood by considering a horizontal line node gap along with large in-plane anisotropy in v_F and the Pauli-paramagnetic effect. The present results shed fresh light on a possibility that the gap symmetry possesses horizontal line nodes and challenge the current view of the order parameter of Sr_2RuO_4 .

These features can be understood by considering a horizontal line node gap along with large in-plane anisotropy in v_F and the Pauli-paramagnetic effect. The present results shed fresh light on a possibility that the gap symmetry possesses horizontal line nodes and challenge the current view of the order parameter of Sr_2RuO_4 .

Acknowledgments We thank Y. Yoshida and H. Yaguchi for their support with the experiments. We also thank Y. Maeno and S. Yonezawa for the fruitful discussion. A part of the numerical calculations was performed by using the HOKUSAI supercomputer system in RIKEN. This work was supported by a Grant-in-Aid for Scientific Research on Innovative Areas “J-Physics” (15H05883, 18H04306) from MEXT and KAKENHI (18H01161, 15K05158, 15H03682, 26400360, 15K17715, 15J05698, 17K05553, 18K04715) from JSPS.

- 1) Y. Maeno, H. Hashimoto, K. Yoshida, S. Nishizaki, T. Fujita, J. G. Bednorz, and F. Lichtenberg, *Nature (London)* **372**, 532 (1994).
- 2) K. Ishida, H. Mukuda, Y. Kitaoka, K. Asayama, Z. Q. Mao, Y. Mori, and Y. Maeno, *Nature (London)* **396**, 658 (1998).
- 3) J. A. Duffy, S. M. Hayden, Y. Maeno, Z. Q. Mao, J. Kulda, and G. J. McIntyre, *Phys. Rev. Lett.* **85**, 5412 (2000).
- 4) K. Ishida, H. Murakawa, H. Mukuda, Y. Kitaoka, Z. Q. Mao, and Y. Maeno, *J. Phys. Chem. Solids* **69**, 3108 (2008).
- 5) K. Ishida, M. Manago, T. Yamanaka, H. Fukazawa, Z. Q. Mao, Y. Maeno, and K. Miyake, *Phys. Rev. B* **92**, 100502(R) (2015).
- 6) A. P. Mackenzie and Y. Maeno, *Rev. Mod. Phys.* **75**, 657 (2003).
- 7) Y. Maeno, S. Kittaka, T. Nomura, S. Yonezawa, and K. Ishida, *J. Phys. Soc. Jpn.* **81**, 011009 (2012).
- 8) G. M. Luke, Y. Fudamoto, K. M. Kojima, M. I. Larkin, J. Merrin, B. Nachumi, Y. J. Uemura, Y. Maeno, Z. Q. Mao, Y. Mori, H. Nakamura, and M. Sigrist, *Nature (London)* **394**, 558 (1998).
- 9) J. Xia, Y. Maeno, P. T. Beyersdorf, M. M. Fejer, and A. Kapitulnik, *Phys. Rev. Lett.* **97**, 167002 (2006).
- 10) C. Bergemann, A. P. Mackenzie, S. R. Julian, D. Forsythe, and E. Ohmichi, *Adv. Phys.* **52**, 639 (2003).
- 11) A. Damascelli, D. H. Lu, K. M. Shen, N. P. Armitage, F. Ronning, D. L. Feng, C. Kim, Z. X. Shen, T. Kimura, Y. Tokura, Z. Q. Mao, and Y. Maeno, *Phys. Rev. Lett.* **85**, 5194 (2000).
- 12) A. P. Mackenzie, T. Scaffidi, C. W. Hicks, and Y. Maeno, *npj Quantum Materials* **2**, 40 (2017).
- 13) S. Yonezawa, T. Kajikawa, and Y. Maeno, *Phys. Rev. Lett.* **110**, 077003 (2013).
- 14) S. Yonezawa, T. Kajikawa, and Y. Maeno, *J. Phys. Soc. Jpn.* **83**, 083706 (2014).
- 15) S. Kittaka, A. Kasahara, T. Sakakibara, D. Shibata, S. Yonezawa, Y. Maeno, K. Tenya, and K. Machida, *Phys. Rev. B* **90**, 220502(R) (2014).
- 16) N. Kikugawa, T. Terashima, S. Uji, K. Sugii, Y. Maeno, D. Graf, R. Baumbach, and J. Brooks, *Phys. Rev. B* **93**, 184513 (2016).
- 17) S. Nishizaki, Y. Maeno, and Z. Q. Mao, *J. Phys. Soc. Jpn.* **69**, 572 (2000).
- 18) M. Suzuki, M. A. Tanatar, N. Kikugawa, Z. Q. Mao, Y. Maeno, and T. Ishiguro, *Phys. Rev. Lett.* **88**, 227004 (2002).
- 19) I. Bonalde, B. D. Yanoff, M. B. Salamon, D. J. van Harlingen, E. M. E. Chia, Z. Q. Mao, and Y. Maeno, *Phys. Rev. Lett.* **85**, 4775 (2000).
- 20) K. Ishida, H. Mukuda, Y. Kitaoka, Z. Q. Mao, Y. Mori, and Y. Maeno, *Phys. Rev. Lett.* **84**, 5387 (2000).
- 21) K. Izawa, H. Takahashi, H. Yamaguchi, Y. Matsuda, M. Suzuki, T. Sasaki, T. Fukase, Y. Yoshida, R. Settai, and Y. Onuki, *Phys. Rev. Lett.* **86**, 2653 (2001).
- 22) M. A. Tanatar, M. Suzuki, S. Nagai, Z. Q. Mao, Y. Maeno, and T. Ishiguro, *Phys. Rev. Lett.* **86**, 2649 (2001).
- 23) K. Deguchi, Z. Q. Mao, H. Yaguchi, and Y. Maeno, *Phys. Rev. Lett.* **92**, 047002 (2004).
- 24) K. Deguchi, Z. Q. Mao, and Y. Maeno, *J. Phys. Soc. Jpn.* **73**, 1313 (2004).

- 25) E. Hassinger, P. Bourgeois-Hope, H. Taniguchi, S. R. de Cotret, G. Grissonnanche, M. S. Anwar, Y. Maeno, N. Doiron-Leyraud, and L. Taillefer, *Phys. Rev. X* **7**, 011032 (2017).
- 26) T. Sakakibara, S. Kittaka, and K. Machida, *Rep. Prog. Phys.* **79**, 094002 (2016).
- 27) Y. Matsuda, K. Izawa, and I. Vekhter, *J. Phys.: Condens. Matter* **18**, R705 (2006).
- 28) A. Vorontsov and I. Vekhter, *Phys. Rev. Lett.* **96**, 237001 (2006).
- 29) M. Hiragi, K. M. Suzuki, M. Ichioka, and K. Machida, *J. Phys. Soc. Jpn.* **79**, 094709 (2010).
- 30) K. An, T. Sakakibara, R. Settai, Y. Ōnuki, M. Hiragi, M. Ichioka, and K. Machida, *Phys. Rev. Lett.* **104**, 037002 (2010).
- 31) S. Kittaka, Y. Aoki, N. Kase, T. Sakakibara, T. Saito, H. Fukazawa, Y. Kohori, K. Kihou, C. H. Lee, A. Iyo, H. Eisaki, K. Deguchi, N. K. Sato, Y. Tsutsumi, and K. Machida, *J. Phys. Soc. Jpn.* **83**, 013704 (2014).
- 32) Z. Q. Mao, Y. Maeno, and H. Fukazawa, *Mat. Res. Bull.* **35**, 1813 (2000).
- 33) A. P. Mackenzie, R. K. W. Haselwimmer, A. W. Tyler, G. G. Lonzarich, Y. Mori, S. Nishizaki, and Y. Maeno, *Phys. Rev. Lett.* **80**, 161 (1998).
- 34) K. Ishida, H. Mukuda, Y. Kitaoka, Z. Q. Mao, H. Fukazawa, and Y. Maeno, *Phys. Rev. B* **63**, 060507(R) (2001).
- 35) H. Murakawa, K. Ishida, K. Kitagawa, Z. Q. Mao, and Y. Maeno, *Phys. Rev. Lett.* **93**, 167004 (2004).
- 36) If the field-independent term of non-electronic contributions is adjusted by assuming that C_e/T of Sr_2RuO_4 in the normal state remains constant,¹⁷⁾ the absolute value of C_e/T also becomes comparable to a previous report.²³⁾
- 37) Z. Q. Mao, Y. Maeno, S. NishiZaki, T. Akima, and T. Ishiguro, *Phys. Rev. Lett.* **84**, 991 (2000).
- 38) H. Yaguchi, T. Akima, Z. Mao, Y. Maeno, and T. Ishiguro, *Phys. Rev. B* **66**, 214514 (2002).
- 39) G. E. Volovik, *JETP Lett.* **58**, 469 (1993).
- 40) F. Bouquet, Y. Wang, I. Sheikin, T. Plackowski, A. Junod, S. Lee, and S. Tajima, *Phys. Rev. Lett.* **89**, 257001 (2002).
- 41) F. Hardy, R. Eder, M. Jackson, D. Aoki, C. Paulsen, T. Wolf, P. Burger, A. Böhmer, P. Schweiss, P. Adelman, R. A. Fisher, and C. Meingast, *J. Phys. Soc. Jpn.* **83**, 014711 (2014).
- 42) From the present data, we cannot distinguish the oscillation pattern in details, *e.g.*, $\cos(4\phi)$ and $1 - 2|\sin(2\phi)|$,²³⁾ which contains useful information on the gap anisotropy.
- 43) (Supplemental Material) (I) Results of $C(\theta)$ measurements on Sr_2RuO_4 , and (II) Pauli-paramagnetic effect on $A_4(H)$ are provided online.
- 44) In recent studies on URu_2Si_2 ⁶⁰⁾ and UPd_2Al_3 ,⁶¹⁾ evidence for the presence of horizontal line nodes has been successfully provided from $C(\theta)$ measurements, which have also been theoretically supported.⁶²⁾
- 45) I. Vekhter and A. Vorontsov, *Physica B* **403**, 958 (2008).
- 46) K. Machida, K. Irie, K. Suzuki, Y. Tsutsumi, and H. Ikeda, unpublished.
- 47) A. Steppke, L. Zhao, M. E. Barber, T. Scaffidi, F. Jerzembeck, H. Rosner, A. S. Gibbs, Y. Maeno, S. H. Simon, A. P. Mackenzie, and C. W. Hicks, *Science* **355**, eaaf9398 (2017).
- 48) Recent experiment of scanning tunneling spectroscopy evaluated $v_{F||[110]}/v_{F||[100]} \approx 0.7$ for the β band.⁶³⁾
- 49) I. Vekhter, P. J. Hirschfeld, J. P. Carbotte, and E. J. Nicol, *Phys. Rev. B* **59**, R9023 (1999).
- 50) P. Miranović, M. Ichioka, K. Machida, and N. Nakai, *J. Phys.: Condens. Matter* **17**, 7971 (2005).
- 51) Y. Amano, M. Ishihara, M. Ichioka, N. Nakai, and K. Machida, *Phys. Rev. B* **90**, 144514 (2014).
- 52) M. Ichioka and K. Machida, *Phys. Rev. B* **76**, 064502 (2007).
- 53) K. Machida and M. Ichioka, *Phys. Rev. B* **77**, 184515 (2008).
- 54) $A_4(T, H)$ at finite μ has been evaluated from the data calculated with $\mu = 0$ by using the universal scaling relation $[dN(E)/dE]_{E=0} \propto 1 - N(E=0)$.⁴⁶⁾
- 55) K. M. Suzuki, Y. Tsutsumi, N. Nakai, M. Ichioka, and K. Machida, *J. Phys. Soc. Jpn.* **80**, 123706 (2011).
- 56) S. Kittaka, T. Nakamura, Y. Aono, S. Yonezawa, K. Ishida, and Y. Maeno, *Phys. Rev. B* **80**, 174514 (2009).
- 57) The α and β bands have relatively small anisotropy in the amplitude of the in-plane v_F ⁴⁷⁾ but have large anisotropy in its orientation, reflecting the quasi-one-dimensional nature. This anisotropy also causes an oscillation of $C_e(\phi = 0^\circ) < C_e(\phi = 45^\circ)$ if horizontal line nodes exist.⁴⁶⁾
- 58) M. E. Zhitomirsky and T. M. Rice, *Phys. Rev. Lett.* **87**, 057001 (2001).
- 59) S. Kunkemöller, P. Steffens, P. Link, Y. Sidis, Z. Q. Mao, Y. Maeno, and M. Braden, *Phys. Rev. Lett.* **118**, 147002 (2017).
- 60) S. Kittaka, Y. Shimizu, T. Sakakibara, Y. Haga, E. Yamamoto, Y. Ōnuki, Y. Tsutsumi, T. Nomoto, H. Ikeda, and K. Machida, *J. Phys. Soc. Jpn.* **85**, 033704 (2016).
- 61) Y. Shimizu, S. Kittaka, T. Sakakibara, Y. Tsutsumi, T. Nomoto, H. Ikeda, K. Machida, Y. Homma, and D. Aoki, *Phys. Rev. Lett.* **117**, 037001 (2016).
- 62) Y. Tsutsumi, T. Nomoto, H. Ikeda, and K. Machida, *Phys. Rev. B* **94**, 224503 (2016).
- 63) Z. Wang, D. Walkup, P. Derry, T. Scaffidi, M. Rak, S. Vig, A. Kogar, I. Zeljkovic, A. Husain, L. H. Santos, Y. Wang, A. Damascelli, Y. Maeno, P. Abbamonte, E. Fradkin, and V. Madhavan, *Nat. Phys.* **13**, 799 (2017).

Supplemental Material for
Searching for gap zeros in Sr_2RuO_4 via field-angle-dependent specific-heat measurement

Shunichiro Kittaka,¹ Shota Nakamura,¹ Toshiro Sakakibara,¹ Naoki Kikugawa,² Taichi Terashima,² Shinya Uji,^{2,3}
 Dmitry A. Sokolov,⁴ Andrew P. Mackenzie,⁴ Koki Irie,⁵ Yasumasa Tsutsumi,^{6,7} Katsuhiko Suzuki,⁸ and Kazushige Machida⁵

¹*Institute for Solid State Physics, University of Tokyo, Kashiwa, Chiba 277-8581, Japan*

²*National Institute for Materials Science, 3-13 Sakura, Tsukuba, Ibaraki 305-0003, Japan*

³*Graduate School of Pure and Applied Sciences, University of Tsukuba, Tsukuba, Ibaraki 305-8577, Japan*

⁴*Max Planck Institute for Chemical Physics of Solids, Nothnitzer Str. 40, 01187 Dresden, Germany*

⁵*Department of Physics, Ritsumeikan University, Kusatsu, Shiga 525-8577, Japan*

⁶*Department of Basic Science, The University of Tokyo, Meguro, Tokyo 153-8902, Japan*

⁷*Condensed Matter Theory Laboratory, RIKEN, Wako, Saitama 351-0198, Japan*

⁸*Research Organization of Science and Technology, Ritsumeikan University, Kusatsu, Shiga 525-8577, Japan*

1. Out-of-plane field-angle dependence of the specific heat for Sr_2RuO_4

Figure S1 shows $C_e(H)/T$ of Sr_2RuO_4 measured at 0.06 K in $H \parallel [001]$. At low fields, $C_e(H)$ measured after the zero-field-cooling process is nearly unchanged up to $\mu_0 H_{c1}$ (~ 7 mT for $H \parallel [001]$) and rapidly increases above H_{c1} . By contrast, $C_e(H)$ measured in the each-point-field-cooling (EPFC) process¹⁾ varies proportionally from 0 T to H . This H -linear behavior is probably due to an increase of trapped fluxes inside the sample. These effects unfortunately mask low-energy quasiparticle excitations in $H \parallel [001]$, in sharp contrast to $C_e(H)$ in $H \parallel ab$; it is expected that $C_e(H)$ increases in proportion to \sqrt{H} in $H \parallel [001]$ if the gap has line nodes.

To explore the out-of-plane gap anisotropy, we investigated the polar-angle θ dependence of the specific heat at 0.06 K under a rotating field within the (010) plane ($\phi = 0^\circ$). First, we measured $C_e(\theta)$ while keeping the sample at a temperature well below 1.5 K (*i.e.*, not in the EPFC process). Then, we found that the results strongly depend on the rotational direction of H ; this is indicated in Fig. S2(a) by solid and dashed lines that represent the data taken in increasing and decreasing θ sweeps, respectively. The dependence on the rotational direction becomes prominent at lower fields. This can be attributed to the strong trap of the magnetic flux, which is illustrated in Fig. S1. Therefore, to align the trapped fluxes with the applied field orientation, we then performed EPFC measurements of $C_e(\theta)$; *i.e.*, the sample temperature once increases well above T_c after each field rotation. EPFC data of $C_e(\theta)$ [symbols in Fig. S2(a)] become symmetric around $\theta = 90^\circ$ with no rotational-direction dependence.

In Fig. S2(b), the EPFC data of $C_e(\theta)$ at various fields are plotted as a function of $H_{\parallel c} = H \cos \theta$, together with the EPFC data of $C_e(\theta = 0, H)$. Except near $H_{\parallel c} \sim 0$, all $C_e(\theta, H)$ data are scaled by $H_{\parallel c}$, and the scaling function matches $C_e(\theta = 0, H)$ well. This means that it is difficult to investigate the out-of-plane gap anisotropy of Sr_2RuO_4 from $C_e(\theta)$ measurements because of the large anisotropy of the coherence length.

2. Pauli-paramagnetic effect on $A_4(H)$

Figure S3 compares $A_4(H)$ obtained from calculations with (squares; $\mu = 0.04$) and without (triangles; $\mu = 0$) the Pauli-paramagnetic effect by assuming a horizontal line node gap and a large in-plane v_F anisotropy. Inclusion of the Pauli-paramagnetic effect tends to shift a hump in $A_4(H)$ toward a higher field. In the case of no Pauli-paramagnetic effect, $A_4(H)$ starts to decrease when the magnetic field exceeds $\sim 0.3H_{c2}$. This behavior is in contrast to the experimental result at 0.1 K (circles in Fig. S3). In addition, a rapid increase in $C_e(H)$ with approaching H_{c2} cannot be reproduced if $\mu = 0$ is adopted. Thus, the Pauli-paramagnetic effect is favorable to explain the specific-heat behavior under a magnetic field.

1) D. Shibata, H. Tanaka, S. Yonezawa, T. Nojima, and Y. Maeno, Phys. Rev. B **91**, 104514 (2015).

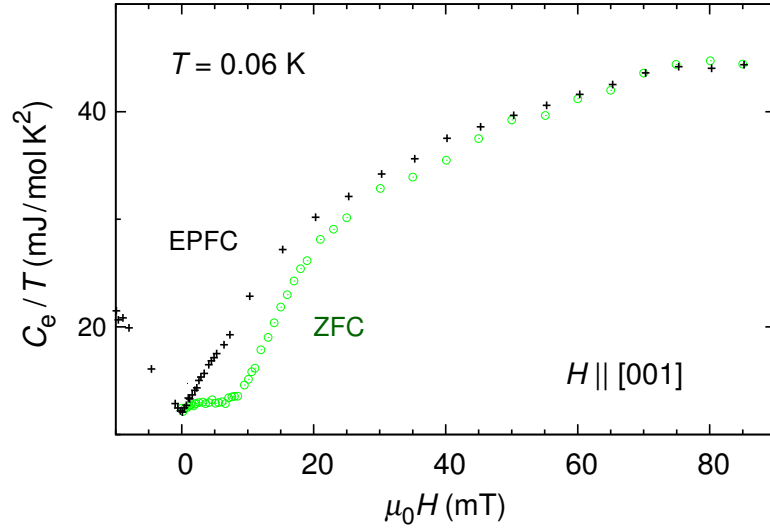


Fig. S1. $C_e(H)/T$ at 0.06 K in $H \parallel [001]$ measured in the zero-field-cooling (ZFC; circles) and each-point-field-cooling (EPFC; crosses) processes.

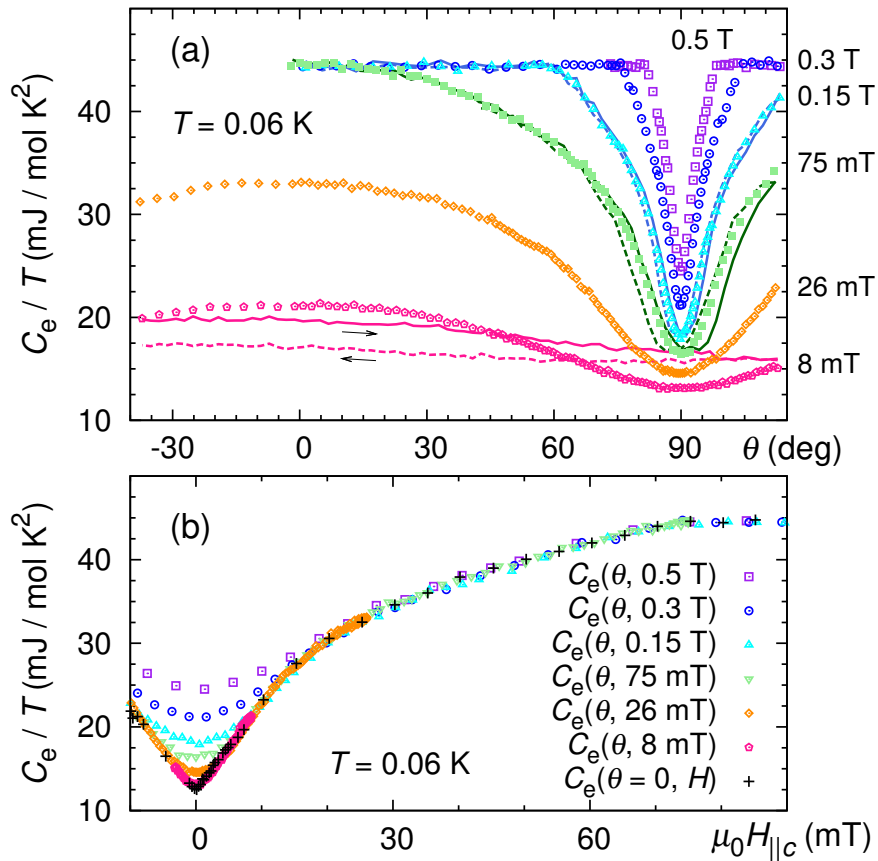


Fig. S2. (a) Field-angle θ dependence of C_e/T at 0.06 K in a rotating magnetic field within the (010) plane. Here, θ denotes the field angle with respect to the [001] axis. Symbols are the data taken in the EPFC process. Solid and dashed lines are the data (8, 75, and 150 mT) taken in the increasing and decreasing θ sweeps, respectively, without increasing the sample temperature significantly. (b) The same data (symbols), as in (a), plotted as a function of the magnetic-field component along the [001] axis, $H_{\parallel c} (= H \cos \theta)$. The EPFC $C_e(H)/T$ data in $H \parallel [001]$ ($\theta = 0$; crosses) are also plotted for comparison.

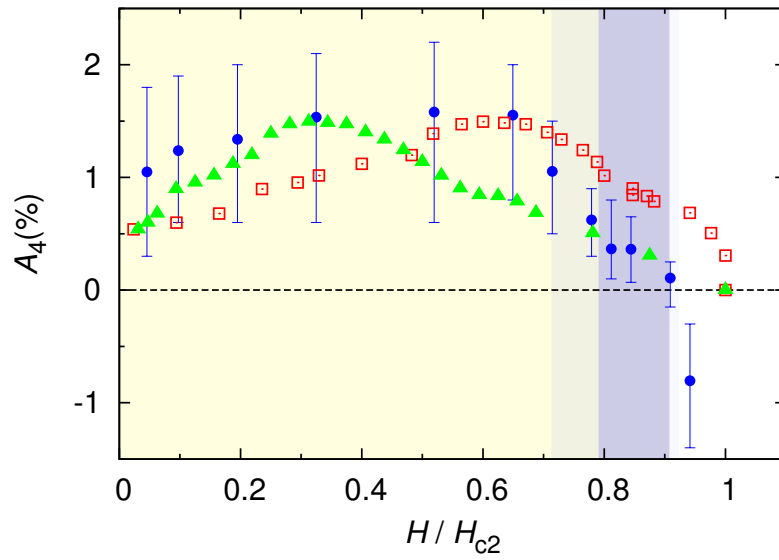


Fig. S3. Field dependence of A_4 calculated with $\mu = 0$ (triangles) and $\mu = 0.04$ (squares) by assuming a horizontal line node gap and a large in-plane v_F anisotropy ($b = 0.5$). Circles are the experimental data at 0.1 K.